

COMMUNICATION

Observing Folding Pathways and Kinetics of a Single Sodium-proton Antiporter from *Escherichia coli***Alexej Kedrov¹, Harald Janovjak, Christine Ziegler², Werner Kuhlbrandt² and Daniel J. Muller^{1*}**¹Center of Biotechnology
University of Technology
01307 Dresden, Germany²Max Planck Institute of
Biophysics, 60439 Frankfurt
Germany

Mechanisms of folding and misfolding of membrane proteins are of interest in cell biology. Recently, we have established single-molecule force spectroscopy to observe directly the stepwise folding of the Na⁺/H⁺ antiporter NhaA from *Escherichia coli* *in vitro*. Here, we improved this approach significantly to track the folding intermediates of a single NhaA polypeptide forming structural segments such as the Na⁺-binding site, transmembrane α -helices, and helical pairs. The folding rates of structural segments ranged from 0.31 s⁻¹ to 47 s⁻¹, providing detailed insight into a distinct folding hierarchy of an unfolded polypeptide into the native membrane protein structure. In some cases, however, the folding chain formed stable and kinetically trapped non-native structures, which could be assigned to misfolding events of the antiporter.

© 2005 Elsevier Ltd. All rights reserved.

Keywords: atomic force microscopy; single-molecule force spectroscopy; sodium/proton antiporter; folding kinetics; molecular interactions

*Corresponding author

The last decade has seen a rapid increase in our understanding of the folding mechanisms of many globular proteins.¹ By contrast, far less progress has been made in folding studies on membrane proteins, which focused mostly on a few well-known model proteins.^{2,3} Major difficulties for intensive studies on integral membrane proteins arise because they are considerably more difficult to work with compared to water-soluble proteins. This is mainly due to difficulties in mimicking the native, anisotropic environment of the cell membrane, where specific interactions are required for the precise folding of hydrophobic residues into functional structures.^{2,4–6} Current folding studies predominantly use conventional bulk techniques, which allow probing average conformational characteristics of molecules in the ensemble, but cannot resolve specific pathways adopted by individual membrane proteins. Recently, single-molecule approaches have demonstrated their potential for observing functionally related

conformations and unfolding pathways of single molecules.^{7–10} Single-molecule force spectroscopy using atomic force microscopy (AFM) has provided detailed insights into molecular interactions related to the structure and function of different biomacromolecules.^{11–14}

Recently, we applied AFM to observe the insertion of single unfolded polypeptide chains of the Na⁺/H⁺ antiporter NhaA of *Escherichia coli*¹⁵ into the membrane and their self-assembly into the folded membrane protein.¹⁶ Here, we refine the method by introducing an improved set-up, which allows determination of the folding kinetics of individual secondary structure elements down to a few milliseconds. After immobilizing membranes containing NhaA on mica, their surfaces were imaged in buffered solution by AFM. Then individual molecules were tethered with their C-terminal end to the AFM tip, which was separated from the membrane with sub-nanometer precision at the speed of 1 μ m/s. Mechanical pulling of the polypeptide resulted in sequential unfolding of all NhaA structural segments, except the last helical pair (α -helices I and II) serving as an anchor of the polypeptide in the membrane. The recorded force–distance (F–D) traces were shown to be highly reproducible and specific for NhaA

Abbreviations used: AFM, atomic force microscopy; F–D, force–distance; k_{fold} , folding rate; NhaA, sodium/proton antiporter; WLC, worm-like chain.

E-mail address of the corresponding author: mueller@biotec.tu-dresden.de

molecules.^{16,17} Each force peak of the F–D trace (Figure 1(a), red curves) represented a single unfolding event. On fitting with the worm-like chain (WLC) model (Figure 1(a), black curves),¹⁸ the peaks were assigned unambiguously to molecular interactions that stabilized certain structural segments of NhaA.¹⁶

After this, the polypeptide was relaxed for a certain length of time to allow refolding (Figure 1(b)). An F–D spectrum recorded while repeatedly pulling the folded peptide exhibited individual force peaks, indicating that the peptide has folded and established certain molecular interactions (Figure 1(a)). Comparing the force spectra of the repeatedly pulled protein with those recorded upon initial unfolding showed that in both

cases the force peaks occurred at the same characteristic position. Since these force peaks are both a measure of molecular interactions and locate these interactions within the native NhaA structure, it was assumed that these parts of the peptide refolded into their structure as established in the functional protein.¹⁶

By improving the AFM detection and feedback system, we reduced the dead-time between the subsequent steps of the experiment to less than 10 ms, which lies below the folding times detected for α -helices of membrane proteins.¹⁹ We therefore assume that the NhaA folds after the peptide is positioned close to the membrane surface and relaxes (Figure 1(b)). In our experiments, we did not observe a snap-in upon relaxation of the

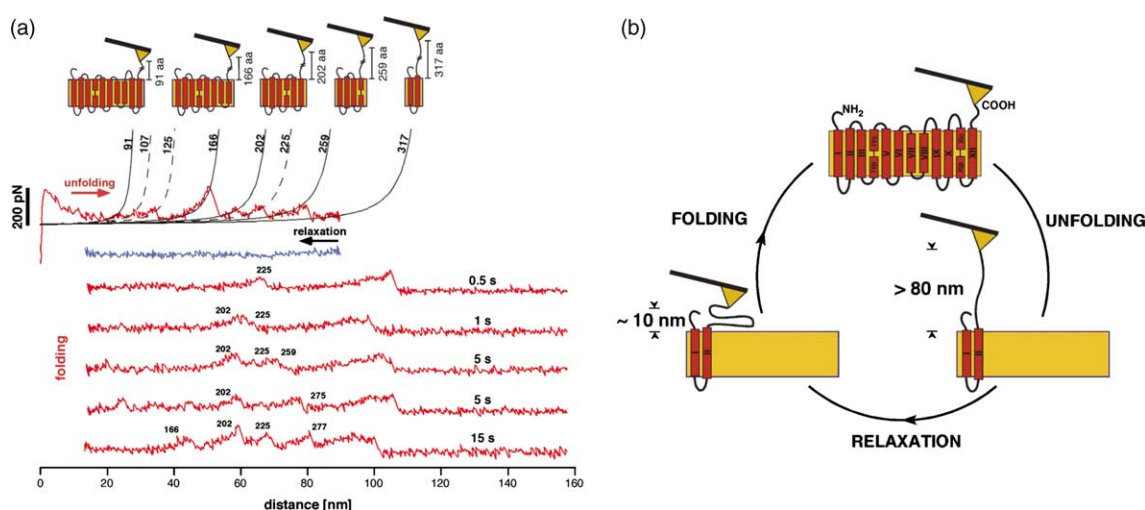


Figure 1. Single-molecule unfolding and refolding of NhaA. (a) Mechanical unfolding of NhaA yielded F–D curves containing characteristic peaks (upper red trace). WLC fits of major (100% occurrence upon initial unfolding) and side force peaks (less than 100% occurrence) are shown by continuous and broken black lines, respectively. The contour length (residues) of the polypeptide chain stretched is given at the end of each fit. The major unfolding pathway of NhaA is shown schematically. F–D curves recorded after certain refolding times are shown in red. Numbers of force peaks give their contour lengths. (b) Scheme of a refolding experiment. Initially, the intact NhaA molecule was unfolded (upper red trace in (a)). The tip was separated from the membrane up to ≈ 80 nm so that the last helical pair remained anchored in the membrane. Then the stretched polypeptide was relaxed as the tip was brought into proximity (≈ 10 nm) of the surface ((a) blue trace). After a specified delay time, the polypeptide was pulled repeatedly while recording an F–D trace ((a) red traces). After certain refolding times, the force peaks detected of the refolded peptide occur at positions identical with those measured upon initial unfolding of NhaA. Since this spectrum exhibits the characteristic unfolding peaks of native NhaA, it follows that the peptide folded into the native structure. As described,³⁵ solubilized NhaA molecules have been reconstituted into a lipid bilayer in which the proteins assembled into two-dimensional crystals exhibiting unit cell dimensions of $48 \text{ \AA} \times 181 \text{ \AA}$ and a $P22_12_1$ symmetry. This suspension was diluted in immobilization buffer (300 mM KCl, 10% (v/v) glycerol, 25 mM potassium acetate (pH 4.0)) to a final protein concentration of $\approx 0.5 \text{ \mu g/ml}$. From this, a 20 \mu l drop was adsorbed onto freshly cleaved mica for 30 min. After this, the mica was rinsed gently with the immobilization buffer (containing no biological samples) to remove weakly attached membranes. AFM experiments were performed in 150 mM KCl, 50 mM NaCl, 20 mM citric acid, pH 4.0. The AFM used (PicoForce, DI-Veeco, Santa Barbara) was equipped with a closed-loop Z-axis. The experiments were performed using 200 \mu m long Si_3N_4 AFM cantilevers (nominal spring constant 0.06 N/m ; DI-Veeco). The thermal noise of cantilevers was measured in solution and spring constants were calculated using the equipartition theorem.^{36,37} We attached single NhaA molecules to the AFM tip by non-specific interactions. This has led to a distribution of observed contour lengths due to pulling molecules from different attachment sites. Only events that demonstrated the characteristic unfolding spectra upon first pulling and exhibited a final contour length of ≈ 100 nm were subjected to further analysis.¹⁶ For data analysis, we focused only on NhaA being unfolded by pulling from its C-terminal end, that comprises $\sim 80\%$ of unfolding events.¹⁷ We used the recently resolved atomic structure of NhaA²¹ to assign stable structural segments from the force spectroscopy curves. In two cases, this has led to the modification of stabilizing structural segments,¹⁶ which were previously assigned on the basis of the predicted secondary structural model.³⁸ The force peak at residue 318 now fits perfectly to the cytoplasmic end of α -helix II of the refined structural model. Additionally, the peak at residue 328 now reflects unfolding of the structured loop I-II after taking a membrane compensation of 11 residues into account.

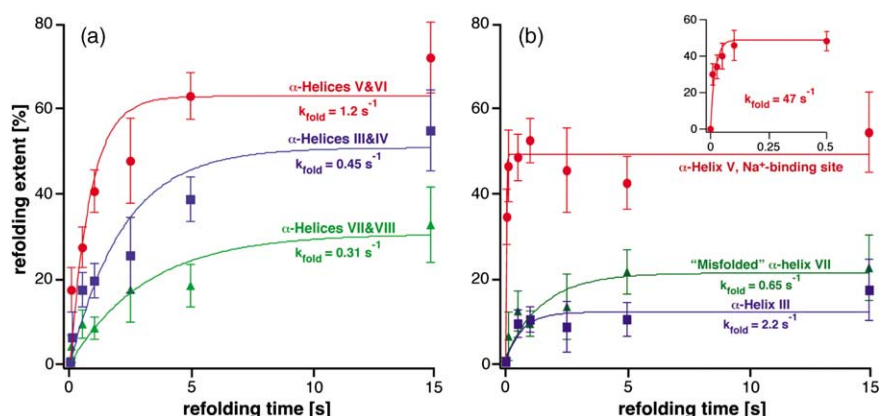


Figure 2. Folding kinetics of structural domains of NhaA. Force peaks detected upon repeated pulling of the NhaA polypeptide were ascribed to refolded structural elements (Figure 1(a)). (a) Folding extent of helical pairs and (b) of single structural segments such as single α -helices or segments thereof. The number of single-molecule refolding events recorded for each time delay was: 52 (10 ms), 54 (30 ms), 48 (50 ms), 38 (100 ms), 84 (500 ms), 97 (1 s), 27 (2.5 s), 51 (5 s), and 28 (15 s). The folding rate, k_{fold} , for every refolded structure was acquired from single-exponential fit (continuous lines) of folding extent: $y = y_0 + A \exp(-t k_{\text{fold}})$. The fastest folding segment of NhaA was the sodium-binding domain of helix V facing the cytoplasm ((b) red; inset). The folding of other protein structures followed after this event. α -Helices of NhaA preferred a pairwise folding pathway.

unfolded peptide (Figure 1(a), relaxation curve), which was previously assigned to a refolding event during relaxation of the polypeptide chain.¹⁶ This refolding event of the unfolded peptide could be observed only in experiments performed at low relaxation speeds ≈ 20 nm/s. The much higher relaxation speed of 2 $\mu\text{m/s}$ of this study did not enable the unfolded NhaA peptide to adopt this conformation, which required a minimum relaxation time of ≈ 30 ms (see Figure 2). To perform experiments with much shorter folding times, the dead-time of the set-up had to be reduced significantly. Therefore, we implemented a one-step voltage pulse, which caused the piezo to make an instant jump and to bring the membrane surface and AFM tip into a close proximity (≈ 10 nm). Due to this improvement, the relaxation time could be reduced to ≈ 3 ms. To this end, the AFM was extended with two server-grade PCs equipped with data acquisition electronics (National Instruments 6110S/6052E, Munich, Germany). While the first PC controlled the piezo position (Igor Pro software, Wavemetrics, Lake Oswego, OR), the second PC recorded the cantilever deflection and Z-sensor data at sampling rates up to 45,000 data points/s. These differences from the previous measurements¹⁶ allowed us to quantify the complete NhaA folding kinetics upon variation of the folding time of the relaxed peptide (Figure 1).

First folding intermediate occurs after 10 ms

About 30% of all F–D traces, which were recorded 10 ms after the tip positioned the unfolded polypeptide at the membrane surface, showed an unfolding peak at a contour length of 65 nm with an average rupture force of $59(\pm 15)$ pN (Figure 1(a)). The reproducibility and high intensity

of the peak suggested that specific bonds were established within this polypeptide region. WLC fitting of the force peak revealed an average contour length of $225(\pm 3)$ residues, which was previously assigned to the domain crucial for sodium binding.^{17,20} This domain hosts the functionally important residues Asp163 and Asp164 within the highly hydrophobic core of α -helix V,²¹ and inserts as a first structural segment into the non-polar lipid bilayer (Figure 1(a)). It was observed recently that this domain is able to refold into the membrane bilayer against an external pulling force of ≈ 50 pN.¹⁶ No other force peak was observed in F–D traces recorded at a refolding time of 10 ms, which reflects the absence of sufficiently strong molecular interactions established within other regions of the polypeptide.

Folding intermediates of first second

Increasing the refolding time to 1 s led to additional force peaks in the F–D traces (Figure 1(a)). Most force peaks occurred at positions that were identical with those that had been assigned previously to unfolding barriers established by structural segments of native NhaA.¹⁶ However, the peaks were detected at lower probability than observed upon initial unfolding of the functional protein (Figure 2). Repeated refolding cycles suggested that variable sets of stable structural segments formed as first folding intermediates. Thus, the molecular interactions at this stage were established independently from each other. Although forces of up to 100 pN were required to rupture the newly built molecular interactions, these forces were, on average, about 30–50% lower than those measured upon initial unfolding of the native protein (Figure 3).

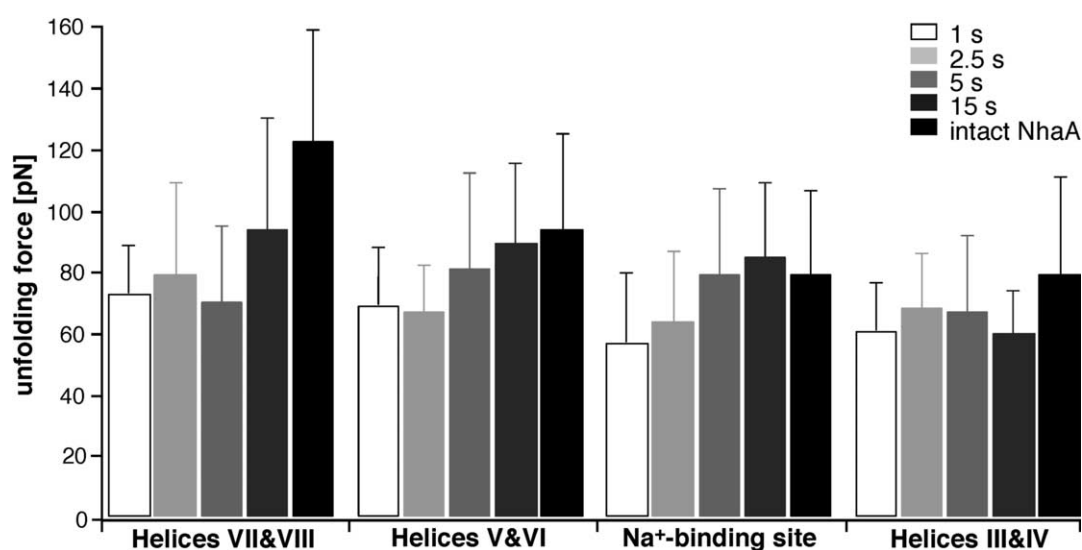


Figure 3. Folding extent determines stability of all structural segments. Average unfolding forces and their standard deviations were measured for refolded structural domains of NhaA. Generally, their stability increased with time given for refolding and, subsequently, with the amount of structures folded. This reflects a critical role of intramolecular interactions in mutual stabilization of the protein domains and formation of its native structure.

Folding intermediates of first 5 s

By relaxing the unfolded polypeptide up to 5 s, the unfolding spectra showed peaks occurring at ≈ 202 and at ≈ 225 residues with probabilities of 60% and 45%, respectively (Figures 1 and 2). This implied that transmembrane α -helices V and VI (202 residues) and the Na⁺-binding site (225 residues)¹⁷ acquired their folded state within the given delay time. In about 35% of all cases, both peaks were observed together in the same spectra, which was in excellent agreement with measurements on unfolding native NhaA.¹⁶ This further suggests that the structural domain has folded correctly. By contrast, the formation of structural segments assigned to the helical pairs III and IV (259 residues) and VII and VIII (166 residues) occurred at the lower probability of 38% and 18%, respectively.

The observation that the formation of the Na⁺-binding site was followed by folding of the embedding helical pair V and VI reflects a rapidly formed folding intermediate. This finding is in agreement with models suggesting that polypeptides can establish a “folding core” within the membrane prior to slower formation of the α -helices.¹⁹ In the case of NhaA, the fast refolding processes suggest that the Na⁺-binding site folds with the highest priority. Currently, it is not clear how the amino acid compositions determine such a priority or hierarchy in folding. In the future, force spectroscopy experiments may be applied on NhaA mutants to investigate this issue in detail. It may be noted here that simple ligand binding to the Na⁺-binding site induces stronger molecular interactions occurring at an enhanced probability.¹⁷ The relatively fast folding kinetics of the helical pair V and VI may be related to its high level of hydrophobicity and the fact that this region contains no proline residue, unlike all other helical pairs of NhaA.²²

Folding proceeded after 15 s

Force peaks corresponding to all structural segments in native NhaA appeared after a folding time of 15 s (Figures 1 and 2). Unfolding forces occurred at values similar to those observed upon initial unfolding (Figure 3). This implies that the molecular interactions stabilizing the molecule consolidated during a period of 15 s. Our experimental data show directly that structural segments established during early folding events formed unfolding barriers at the same positions as in native NhaA, but that their intrinsic stability within the membrane bilayer was lower. With increasing number of structural segments folded, their stability increased as well. This suggests that multiple intramolecular interactions contribute to the stabilization of the functional protein, which is in agreement with conventional folding studies on membrane proteins.²³ Remarkably, it has been found recently that changing the oligomeric assembly of membrane proteins did not influence the location but rather the stability of their structural segments.²⁴ Thus, it can be concluded that an increase in complexity in molecular organization changes the strength of interactions formed by existing structural segments.

Extracting folding kinetics

Folding kinetics of NhaA structural domains were estimated from single-exponential fits to their refolding probabilities at time ranges between 10 ms and 15 s (Figure 2, continuous curves). We excluded α -helices IX–XII from the analysis, as their refolding could be constrained by their close proximity with the AFM tip. The Na⁺-binding region of the polypeptide (around residue 225) demonstrates the highest folding rate of

$47(\pm 19) \text{ s}^{-1}$, suggesting the highest priority of folding. Remarkably, the entire helical pair V and VI folds at a significantly lower rate of $1.2(\pm 0.2) \text{ s}^{-1}$. The helical pairs III and IV, and VII and VIII showed folding rates of the same order of magnitude; $0.45(\pm 0.17) \text{ s}^{-1}$ and $0.31(\pm 0.12) \text{ s}^{-1}$, respectively. A possible schematic folding pathway for a single NhaA may be drawn from these folding constants. The probability of an individual folding pathway to occur can be derived from the folding kinetics. Most of the measured folding constants were within the range determined for membrane proteins and their fragments by conventional bulk experiments ($0.002\text{--}13 \text{ s}^{-1}$).² The low dead-time of our experimental setup allowed resolving fast formations of folding intermediates. However, the single-molecule experiments showed that the folding rates measured conventionally held only for the average folding process, and that single folding events may exhibit significant differences, leading to various folding pathways. Moreover, our experiments demonstrated that the formation of molecular interactions is not necessarily correlated between different α -helical pairs and suggested independent folding of helical pairs.

α -Helices may fold individually or pairwise with neighboring helices, and we observed several folding intermediates and pathways. However, our data suggest that it is more probable that α -helices insert pairwise than their folding as individual units (Figure 2). For example, after a folding time of 15 s, less than 10% of F–D curves contained peaks that could be assigned to the single transmembrane α -helix III (unfolding peak at residue 275), while the pairwise insertion of α -helices III and IV occurred in $\sim 50\%$ cases. Clearly, the formation of helical pairs is the preferable folding pathway of NhaA. This observation is supported by the model describing a pairwise insertion of transmembrane helices as a possible folding pathway, such as that proposed in 1981 by Engelman and Steitz,²⁵ and later confirmed experimentally.^{26–28} In this work, we observed a direct correlation between the folding rate and final refolding extent for individual structural domains of NhaA (Figure 2). Structural domains exhibiting the highest folding kinetics (α -helices V and VI, Na⁺-binding domain) refolded at highest probability ($\approx 50\text{--}60\%$ of all cases). The origin of the trend is not clear, but we are aware that it can be a consequence of the misfolding events discussed below. At the same time, we rule out the influence of experimental drift on the folding process. The setup was equilibrated thermally for 30–60 min prior to the experiments to minimize possible distortions due to cantilever bending, while the piezoelectric actuator was equipped with a maintenance-free capacitive hardware sensor, which ensured stable functioning of the AFM.

Observing misfolding events

Occasionally, the refolded polypeptide showed a peak at residue 180, which was not observed upon

initial unfolding of the native NhaA (Figures 1(a) and 2(b)). The structural segment was formed in $\approx 15\%$ of all cases and showed a folding rate, k_{fold} , of $0.7(\pm 0.4) \text{ s}^{-1}$. There are two possible explanations for this observation: (i) the conformation detected represents a folding intermediate of NhaA along the pathway leading to the functional protein, or (ii) the intermediate is formed due to non-native molecular interactions that trap a misfolded form of the protein in a local energy minimum.²⁹ The absence of kinetics at long timescales (Figure 2(b)) for the structural domain at residue 180 is consistent with a misfolding event. Misfolding events can occur either within the membrane or in the polar environment of membrane–water interface region. We consider that surface misfolding may affect the ability of the peptide to fold spontaneously into the final protein structure. Thus, one may assume that this process is somehow in competition with the insertion of transmembrane domains. The atomic model of NhaA²¹ suggests that the above polypeptide segment forms two short transmembrane α -helices, VII and VIII, of 14 residues each. Since α -helices require at least 20 residues to transverse the lipid bilayer,³⁰ shorter helical regions may account for the observed slow folding kinetics and misfolding events. Alternatively, one may assume that the peptide formed a 3_{10} helix, which needs only ≈ 15 residues to span the membrane bilayer.^{25,31} Nonetheless, our observations demonstrate the ability of single-molecule force measurements to detect different structural states of a membrane protein formed due to alternative molecular interactions.

Various folding pathways guide to native structure

The denatured state of a protein is an operational definition in conventional unfolding approaches, and merely denotes that the protein is inactive but does not define its structure.[†] As suggested for the folding of water-soluble proteins, the conformational differences at the starting point of folding may also initiate different folding pathways of the protein.³² Such differences in reference states should be kept in mind when comparing folding data obtained by different techniques. Controlled unfolding of a membrane protein by AFM defines its fully unfolded state lacking secondary or tertiary interactions (Figure 1), which is comparable to the newly synthesized molecule *in vivo*. Relaxation of the polypeptide chain leads to its rapid coiling in the proximity of the membrane. This compact denatured conformation in the presence of pre-folded helices I and II should be referred to as a protein state prior to the refolding phase in our experiment. The observation of different stable structural segments forming in NhaA within the first second tells us that there are various intermediates through which the membrane protein folding pathway proceeds, even though the experimental conditions were identical for every

unfolded peptide. These intermediates may act as nucleation sites for further folding events.¹ Clearly, detailed studies of membrane protein folding and insertion pathways *in vitro* can shed light on processes in the living cell, such as Sec-independent insertion/translocation of polypeptides in the cell membrane.³³ It was discovered recently that the probability of a given unfolding pathway of a membrane protein depends on external conditions such as temperature, electrolyte or functional state of the protein.^{17,34} We assume that there are various pathways by which a membrane protein can unfold, as well as various pathways of folding. It will be interesting to investigate how environmental conditions or point mutations will affect the folding process of membrane proteins, and how distinct folding pathways leading to misfolding and mal-function can be avoided.

Acknowledgements

We thank Tanuj Sapra for critical reading and valuable discussions. The Deutsche Volkswagenstiftung, the Deutsche Forschungsgemeinschaft, the European Union and the Free State of Saxony supported this work.

References

- Daggett, V. & Fersht, A. (2003). The present view of the mechanism of protein folding. *Nature Rev. Mol. Cell. Biol.* **4**, 497–502.
- Booth, P. J. (2000). Unravelling the folding of bacteriorhodopsin. *Biochim. Biophys. Acta*, **1460**, 4–14.
- Engelman, D. M., Chen, Y., Chin, C. N., Curran, A. R., Dixon, A. M., Dupuy, A. D. *et al.* (2003). Membrane protein folding: beyond the two stage model. *FEBS Letters*, **555**, 122–125.
- White, S. H. & Wimley, W. C. (1999). Membrane protein folding and stability: physical principles. *Annu. Rev. Biophys. Biomol. Struct.* **28**, 319–365.
- Haltia, T. & Freire, E. (1995). Forces and factors that contribute to the structural stability of membrane proteins. *Biochim. Biophys. Acta*, **1241**, 295–322.
- Caffrey, M. (2003). Membrane protein crystallization. *J. Struct. Biol.* **142**, 108–131.
- Medina, M. A. & Schwille, P. (2002). Fluorescence correlation spectroscopy for the detection and study of single molecules in biology. *BioEssays*, **24**, 758–764.
- Mollova, E. T. (2002). Single-molecule fluorescence of nucleic acids. *Curr. Opin. Chem. Biol.* **6**, 823–828.
- Lipman, E. A., Schuler, B., Bakajin, O. & Eaton, W. A. (2003). Single-molecule measurement of protein folding kinetics. *Science*, **301**, 1233–1235.
- Forkey, J. N., Quinlan, M. E., Shaw, M. A., Corrie, J. E. & Goldman, Y. E. (2003). Three-dimensional structural dynamics of myosin V by single-molecule fluorescence polarization. *Nature*, **422**, 399–404.
- Oesterhelt, F., Oesterhelt, D., Pfeiffer, M., Engel, A., Gaub, H. E. & Muller, D. J. (2000). Unfolding pathways of individual bacteriorhodopsins. *Science*, **288**, 143–146.
- Rief, M. & Grubmüller, H. (2002). Force spectroscopy of single biomolecules. *Chem. Phys. Chem.* **3**, 255–261.
- Fernandez, J. M. & Li, H. (2004). Force-clamp spectroscopy monitors the folding trajectory of a single protein. *Science*, **303**, 1674–1678.
- Schwaiger, I., Schleicher, M., Noegel, A. A. & Rief, M. (2005). The folding pathway of a fast-folding immunoglobulin domain revealed by single-molecule mechanical experiments. *EMBO Rep.* **6**, 46–51.
- Taglicht, D., Padan, E. & Schuldiner, S. (1991). Overproduction and purification of a functional Na⁺/H⁺ antiporter coded by nhaA (ant) from *Escherichia coli*. *J. Biol. Chem.* **266**, 11289–11294.
- Kedrov, A., Ziegler, C., Janovjak, H., Kuhlbrandt, W. & Muller, D. J. (2004). Controlled unfolding and refolding of a single sodium-proton antiporter using atomic force microscopy. *J. Mol. Biol.* **340**, 1143–1152.
- Kedrov, A., Krieg, M., Ziegler, C., Kuhlbrandt, W. & Muller, D. J. (2005). Locating ligand binding and activation of a single antiporter. *EMBO Rep.* **6**, 668–674.
- Bustamante, C., Marko, J. F., Siggia, E. D. & Smith, S. (1994). Entropic elasticity of lambda-phage DNA. *Science*, **265**, 1599–1600.
- Riley, M. L., Wallace, B. A., Flitsch, S. L. & Booth, P. J. (1997). Slow alpha helix formation during folding of a membrane protein. *Biochemistry*, **36**, 192–196.
- Inoue, H., Noumi, T., Tsuchiya, T. & Kanazawa, H. (1995). Essential aspartic acid residues, Asp-133, Asp-163 and Asp-164, in the transmembrane helices of a Na⁺/H⁺ antiporter (NhaA) from *Escherichia coli*. *FEBS Letters*, **363**, 264–268.
- Hunte, C., Screpanti, E., Venturi, M., Rimon, A., Padan, E. & Michel, H. (2005). Structure of a Na⁺/H⁺ antiporter and insights into mechanism of action and regulation by pH. *Nature*, **435**, 1197–1202.
- Lu, H., Marti, T. & Booth, P. J. (2001). Proline residues in transmembrane alpha helices affect the folding of bacteriorhodopsin. *J. Mol. Biol.* **308**, 437–446.
- Doi, T., Molday, R. S. & Khorana, H. G. (1990). Role of the intradiscal domain in rhodopsin assembly and function. *Proc. Natl Acad. Sci. USA*, **87**, 4991–4995.
- Sapra, T., Besir, H., Oesterhelt, D. & Muller, D. J. (2005). Mechanisms stabilizing membrane proteins assembled into oligomers. *J. Mol. Biol.* In the press.
- Engelman, D. M. & Steitz, T. A. (1981). The spontaneous insertion of proteins into and across membranes: the helical hairpin hypothesis. *Cell*, **23**, 411–422.
- Kuhn, A. (1987). Bacteriophage M13 procoat protein inserts into the plasma membrane as a loop structure. *Science*, **238**, 1413–1415.
- Saaf, A., Hermansson, M. & von Heijne, G. (2000). Formation of cytoplasmic turns between two closely spaced transmembrane helices during membrane protein integration into the ER membrane. *J. Mol. Biol.* **301**, 191–197.
- Janovjak, H., Struckmeier, J., Hubain, M., Kedrov, A., Kessler, M. & Muller, D. J. (2004). Probing the energy landscape of the membrane protein bacteriorhodopsin. *Structure (Camb)*, **12**, 871–879.
- Sanders, C. R. & Nagy, J. K. (2000). Misfolding of membrane proteins in health and disease: the lady or the tiger? *Curr. Opin. Struct. Biol.* **10**, 438–442.
- Jensen, M. O. & Mouritsen, O. G. (2004). Lipids do influence protein function—the hydrophobic matching hypothesis revisited. *Biochim. Biophys. Acta*, **1666**, 205–226.

31. Ostermeier, C., Harrenga, A., Ermler, U. & Michel, H. (1997). Structure at 2.7 Å resolution of the *Paracoccus denitrificans* two-subunit cytochrome *c* oxidase complexed with an antibody FV fragment. *Proc. Natl Acad. Sci. USA*, **94**, 10547–10553.
32. Shortle, D. (2002). The expanded denatured state: an ensemble of conformations trapped in a locally encoded topological space. *Advan. Protein Chem.* **62**, 1–23.
33. Andersson, H. & von Heijne, G. (1993). Sec dependent and sec independent assembly of *E. coli* inner membrane proteins: the topological rules depend on chain length. *EMBO J.* **12**, 683–691.
34. Janovjak, H., Kessler, M., Oesterhelt, D., Gaub, H. & Muller, D. J. (2003). Unfolding pathways of native bacteriorhodopsin depend on temperature. *EMBO J.* **22**, 5220–5229.
35. Williams, K. A. (2000). Three-dimensional structure of the ion-coupled transport protein NhaA. *Nature*, **403**, 112–115.
36. Butt, H. J. & Jaschke, M. (1995). Calculation of thermal noise in atomic force microscopy. *Nanotechnology*, **6**, 1–7.
37. Florin, E. L., Rief, M., Lehmann, H., Ludwig, M., Dornmair, C., Moy, V. T. & Gaub, H. E. (1995). Sensing specific molecular interactions with the atomic force microscopy. *Biosens. Bioelectron.* **10**, 895–901.
38. Rothman, A., Padan, E. & Schuldiner, S. (1996). Topological analysis of NhaA, a Na⁺/H⁺ antiporter from *Escherichia coli*. *J. Biol. Chem.* **271**, 32288–32292.

Edited by W. Baumeister

(Received 6 July 2005; received in revised form 5 October 2005; accepted 13 October 2005)
Available online 8 November 2005